EVI1 oncoprotein interacts with a large and complex network of proteins and integrates signals through protein phosphorylation

Emilie A. Bard-Chapeau[a], Jayantha Gunaratne[b], Pankaj Kumar[c], Belinda Q. Chua[a], Julius Muller[a], Frederic A. Bard[c], Walter Blackstock[b], Neal G. Copeland[a,1], and Nancy A. Jenkins[a,1,2]

[a]Cancer Genetics Group, [b]Quantitative Proteomics Group, and [c]Cell Structure and Function Group, Institute of Molecular and Cell Biology, Singapore 138673

Contributed by Nancy A. Jenkins, May 17, 2013 (sent for review March 18, 2013)

Ecotropic viral integration site-1 (EVI1) is an oncogenic zinc finger transcription factor whose expression is frequently up-regulated in myeloid leukemia and epithelial cancers. To better understand the mechanisms underlying EVI1-associated disease, we sought to define the EVI1 interactome in cancer cells. By using stable isotope labeling by amino acids in cell culture (SILAC)-based quantitative proteomics, we could confidently assign 78 proteins as EVI1-interacting partners for FLAG-tagged EVI1. Subsequently, we showed that 22 of 27 tested interacting proteins could coimmunoprecipitate with endogenous EVI1 protein, which represented an 81.5% validation rate. Additionally, by comparing the stable isotope labeling by amino acids in cell culture (SILAC) data with high-throughput yeast two hybrid results, we showed that five of these proteins interacted directly with EVI1. Functional classification of EVI1-interacting proteins revealed associations with cellular transcription machinery; modulators of transcription; components of WNT, TGF-β, and RAS pathways; and proteins regulating DNA repair, recombination, and mitosis. We also identified EVI1 phosphorylation sites by MS analysis and showed that Ser538 and Ser858 can be phosphorylated and dephosphorylated by two EVI1 interactome proteins, casein kinase II and protein phosphatase-1α. Finally, mutations that impair EVI1 phosphorylation at these sites reduced EVI1 DNA binding through its C-terminal zinc finger domain and induced cancer cell proliferation. Collectively, these combinatorial proteomic approaches demonstrate that EVI1 interacts with large and complex networks of proteins, which integrate signals from various different signaling pathways important for oncogenesis. Comprehensive analysis of the EVI1 interactome has thus provided an important resource for dissecting the molecular mechanisms of EVI1-associated disease.

MDS1 | EVI1 complex locus mass spectrometry

Ecotropic viral integration site 1 (EVI1) is a zinc finger transcription factor (TF) whose overexpression in acute and chronic myeloid leukemia has been extensively studied and correlated with poor patient survival (1–3). Amplification and/or overexpression of *EVI1* has also been observed in a number of epithelial cancers (4–8), which, in some cases, is significantly associated with cancer aggressiveness and adverse patient outcome (9, 10), indicating that EVI1 is a dominant oncogene important in many types of cancer. EVI1 is one product of the myelodysplasia syndrome-associated protein 1 (MDS1) and EVI1 complex locus (*MECOM*), which encodes several alternatively spliced transcripts. *EVI1* is the most oncogenic and abundant isoform expressed in tumors. It is a 1,051-aa protein containing two zinc finger domains and an acidic C-terminal region (11–13). Other isoforms include a truncated variant, EVI1Δ324, which lacks part of the first zinc finger domain, thus impairing its ability to transform Rat-1 cells (14). A longer variant protein, termed MDS1-EVI1, is a less abundant isoform containing a 188-aa extension at its 5′ end, which adds the so-called PRDI-BF1 and RIZ (PR) homology domain. This protein is thought to function as a tumor suppressor gene rather than an oncogene, and its presence in tumors is associated with good prognosis (9, 15).

Although *EVI1* was discovered in 1988 (16, 17), much remains to be learned about its molecular function and regulation. For instance, only a few EVI1-interacting proteins are currently known. These studies have shown that EVI1 is a dynamic modulator of transcription that can recruit either coactivators or corepressors of transcription, some of which remodel chromatin to further stabilize changes at the epigenetic level (12, 13, 15). In addition, a few TFs such as runt-related transcription factor 1, GATA1, PU.1, FBJ murine osteosarcoma viral oncogene homolog (FOS), and SMAD family member 3 (SMAD 3) have been shown to interact with EVI1 and help transcriptionally regulate events such as hematopoietic differentiation, cell death, and proliferation (18–22).

As part of our continuing effort to characterize the biological functions of EVI1 in normal and tumor cells, we have performed a series of stable isotope labeling by amino acids in cell culture (SILAC)-based proteomics experiments aimed at identifying additional EVI1-binding partners. In these experiments, we isolated EVI1-interacting complexes and performed quantitative proteomics combined with yeast two-hybrid screens. Eight previously known EVI1 interacting proteins were identified in addition to many other interacting partners. The MS results were subsequently validated by coimmunoprecipitation experiments with endogenous EVI1 protein in two different cell lines. Classification of the EVI1 interactome by computational approaches identified a number of protein interaction networks linked to EVI1 and generated a more comprehensive overview of the role of EVI1

Significance

Although ecotropic viral integration site 1 (EVI1) oncogenic transcription factor was discovered in 1988, its molecular functions and regulations are still underexplored. Through characterization of few EVI1-interacting proteins, EVI1 was identified as dynamic modulator of transcription and chromatin remodeling. We used proteomics approaches to define the EVI1 interactome. We found associations of EVI1 with not only transcriptional regulators, but also components of signaling pathways, DNA repair, DNA recombination, and mitosis complexes. We also identified functional EVI1 phosphorylation sites modified by casein-kinase II and protein phosphatase-1α that impact EVI1 activity. Thus, our study provides critical molecular insights on EVI1 action and regulation.

Author contributions: E.A.B.-C., N.G.C., and N.A.J. designed research; E.A.B.-C., J.G., and B.Q.C. performed research; E.A.B.-C., J.G., P.K., J.M., F.A.B., and W.B. contributed new reagents/analytic tools; E.A.B.-C., J.G., P.K., J.M., F.A.B., W.B., N.G.C., and N.A.J. analyzed data; and E.A.B.-C., J.G., N.G.C., and N.A.J. wrote the paper.

The authors declare no conflict of interest.

[1]Present address: Methodist Hospital Research Institute, Houston, TX 77030.

[2]To whom correspondence should be addressed. E-mail: njenkins2@tmhs.org.

This article contains supporting information online at www.pnas.org/lookup/suppl/doi:10.1073/pnas.1309310110/-/DCSupplemental.

in neoplastic disease. Our experiments also showed that EVI1 is targeted by enzymatic complexes such as casein-kinase II (CK2) and protein phosphatase-1α (PP1α), which in turn modulate its DNA binding activity through serine phosphorylation.

Results

Purification of FLAG-EVI1–Interacting Complexes and Quantitative Analysis. To further define the nature of the EVI1 protein complexes present in cancer cells, we first sought to determine the size of these complexes by using gel filtration chromatography. SKOV3 ovarian carcinoma cells were used in these experiments because EVI1 is thought to be an ovarian carcinoma oncogene (9, 18), and, by analyzing the EVI1 protein complexes in these cells, we thus hoped to identify some of the EVI1-binding partners important for neoplastic transformation. In addition, unlike most other cell lines tested, stable EVI1 protein can be transiently expressed in SKOV3 cells, which is critical for the quantitative SILAC MS proteomics experiments described later. After complete removal of DNA from SKOV3 nuclear lysates (Fig. S1*A*), proteins were eluted into 80 different fractions that were subsequently separated by SDS/PAGE. EVI1 eluted only in complexes of a molecular mass greater than 2,000 kDa, showing that, in SKOV3 cells, EVI1 is part of very large multiprotein complexes (Fig. 1*A*).

A powerful means to characterize the EVI1-associated proteins is through the use of quantitative SILAC MS (23) (Fig. 1*B*). Because human *EVI1* encodes multiple alternative splice forms, we decided to transiently express a FLAG-tagged EVI1 protein coding for the full-length isoform (1,051 aa), which is the most abundant and oncogenic of all EVI1 transcript variants (16) in SKOV3 cells. SKOV3 cells express endogenous EVI1 protein and should therefore also express the binding partners for EVI1 (Fig. S1*B*). We then verified that the expressed FLAG-EVI1 protein localized in the chromatin, like EVI1 (Fig. S1*C*). Cells incubated with light isotopes of lysine and arginine (also called "light" or "L" cells) were then transiently transfected with a control FLAG tag plasmid, whereas cells incubated with heavy isotopes of lysine and arginine (called "heavy" or "H" cells) were transiently transfected with a plasmid expressing FLAG-EVI1 (Fig. 1*B*). Equal amounts of nuclear lysates from these two cultures were then used for immunoprecipitation of FLAG or FLAG-EVI1 proteins, respectively, using agarose beads conjugated with FLAG antibody (Fig. S1*B*). The beads from each sample were then combined, washed, and eluted by SDS (Fig. 1*B*). The eluates were subsequently separated by SDS/PAGE (Fig. S1*D*), subjected to in-gel trypsin digestion, and analyzed with the use of a nanoLC Orbitrap MS system.

Identification of FLAG-EVI1 Binding Partners by SILAC MS and Validation by Coimmunoprecipitation with Endogenous EVI1 Protein. SILAC MS made it possible to compare the amounts of proteins immunoprecipitated from cells transfected with FLAG (light) or FLAG-EVI1 (heavy). The integrated intensity sum of the peptide peaks as determined by using MaxQuant reflects the peptide abundance, and the fold change represents the ratio of peptides quantified in the experimental sample labeled with heavy isotopes vs. the control sample labeled with light isotopes. Most of the proteins identified by SILAC MS were present in a 1:1 ratio and therefore likely to represent background protein interactions (Fig. 1*C*). The greater the deviation the peptide ratio is from 1:1, the higher the likelihood they are true EVI1 protein binding partners. By using a very stringent heavy:light ratio of 3:1 (Fig. 1*C*), we found 73 high-confidence EVI1 interacting proteins (Datasets S1 and S2). We also selected five additional proteins identified below the 3:1 cutoff, but known to form complexes with some of the 73 high-confidence EVI1 interacting proteins (Dataset S1). Eight of these 78 proteins have been previously described to be associated with EVI1 including C-terminal binding protein (CtBP) 1 (11, 24); CtBP2 (25); histone deacetylase (HDAC) 1 (26), HDAC2 (24); cAMP responsive element modulator (CREM), closely related to cAMP responsive element binding (CREB) (26); FOS-like 2 (FOSL2); JUNB; and Yin and Yang 1 (YY1) (18). Comparing this list of 78 proteins with the InterPro database for protein domains revealed a statistically significant enrichment for proteins containing domains involved in the regulation of chromatin remodeling, transcription, DNA repair, and signal transduction (Fig. 1*D*), consistent with EVI1's localization to the chromatin (Fig. S1*C*).

To further verify that these are authentic EVI1 binding partners, we picked 35 interactors, eight of which are known EVI1 interactors, for which good antibodies were available, and asked whether they would also coimmunoprecipitate with endogenous EVI1 protein expressed in SKOV3 cells (Fig. 2*A*). Overall, 81.5% of the EVI1 interacting proteins tested coimmunoprecipitated with endogenous EVI1 protein (22 of 27 previously unkown interactors), attesting to the quality of the SILAC MS results (Fig. 2*B*). The dataset also contained five common known MS contaminants (27) that were specifically identified with a ratio cutoff >3:1. Validation experiments, however, showed that two of these proteins [laminA/C and Poly (ADP-Ribose) Polymerase 1 (PARP1)] are EVI1-associated proteins (Fig. S2*A*). A few previously known EVI1 binding partners were not identified in our screen (Dataset S1). The failure to detect these proteins could have resulted from their low abundance or not having MS-amenable tryptic peptides. We therefore performed additional coimmunoprecipitation experiments to assess their binding to EVI1 in SKOV3 cells. SMAD3; SWI/SNF related, matrix associated, actin dependent regulator of chromatin, subfamily a, member 4 (SMARCA4, BRG1); euchromatic histone-lysine N-methyltransferase 2 (EHMT2, G9a); and general control of amino acid synthesis yeast homolog like 2 (GCN5L2) were consistently found to form complexes with EVI1 in SKOV3 cells (Fig. S2*B*). We previously described FOS and JUN in complex with EVI1 in SKOV3 cells (18). DNA mismatch repair proteins MutS protein homolog (MSH) 2 and MSH6 were identified in the SILAC list. Each of them is thought to interact with MSH3 to form MSH2/MSH3 and MSH2/MSH6 tumor suppressor complexes (28). Thus, we attempted to verify the binding of EVI1 with MSH3 (Fig. S2*C*). MSH3 coimmunoprecipitated with endogenous EVI1, indicating that EVI1 interacts with both DNA mismatch repair complexes, MSH2/MSH3 and MSH2/MSH6.

To confirm that these protein interactions also occur under different physiological conditions, we performed coimmunoprecipitation assays for 17 EVI1 binding partners in K562 myeloid leukemia cells, which express EVI1 in lower amounts than SKOV3 cells. We were able to confirm 15 of the 17 tested interactions with endogenous EVI1 expressed in K562 cells (Fig. 2 *C* and *D*). Collectively, these findings demonstrate that EVI1 is part of very large protein complexes, and provide a reliable and comprehensive list of EVI1-associated proteins.

Most EVI1 Interacting Proteins Bind to EVI1 in Region Located Between the Two EVI1 Zinc Finger Domains. The EVI1 interacting proteins identified by SILAC MS could associate with EVI1 through direct or indirect interactions. To identify the proteins that directly interact with EVI1, we made use of the Pronet technology, which involves yeast two-hybrid high-throughput screening in combination with a high-standard quality control (29). Eighteen different baits were designed from EVI1, 11 of which gave rise to significant positive interactions (Fig. S3) in the seven different libraries that were used in independent screens. These two-hybrid mapping experiments identified 51 preys (Fig. 3*A*) representing possible EVI1 direct binding partners. Many of these hits may be false positives, as the yeast two-hybrid methods are known to give high amounts of unspecific bindings and must be followed by validation. Thus, to identify true EVI1 direct interacting proteins, we compared these yeast two-hybrid results

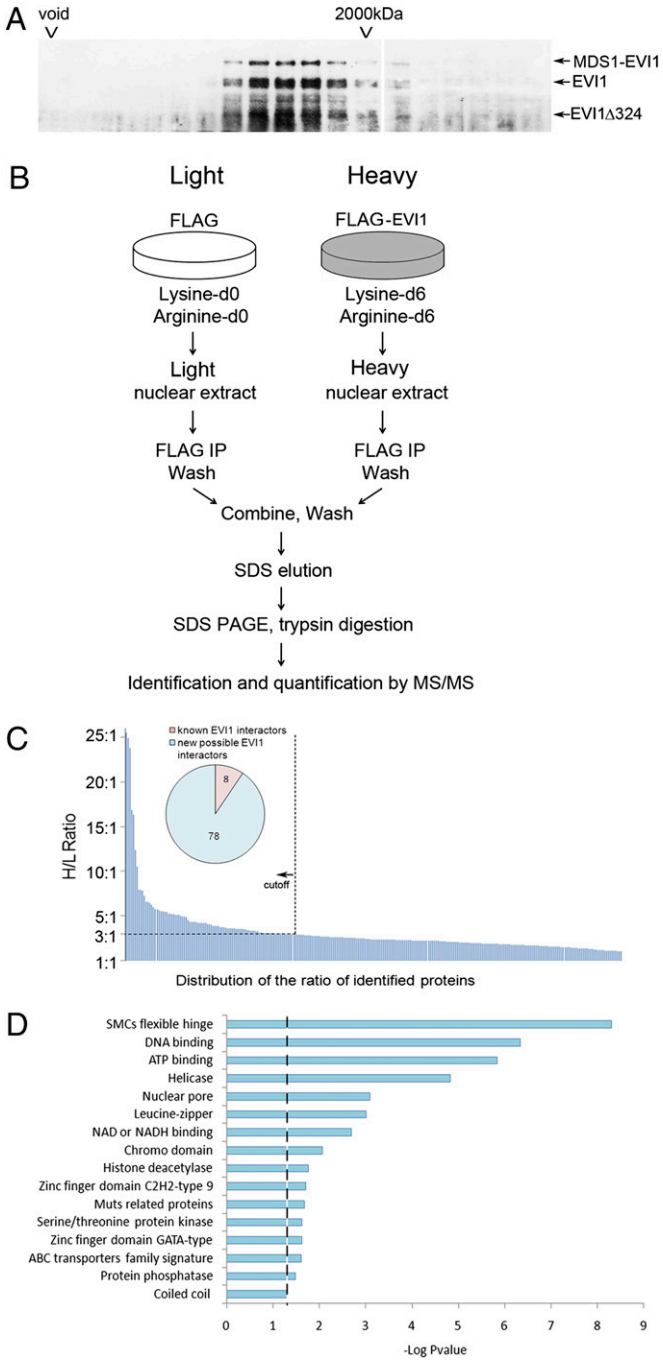

Fig. 1. Quantitative analysis of EVI1 protein complexes. (*A*) Gel filtration analysis of EVI1 protein complexes. A DNA-free and cleared lysate from SKOV3 cells was fractionated by using a Superdex 200 gel filtration column. The fractions were then collected for Western blotting with an anti-EVI1 antibody. Dextran 2,000 kDa was used as a standard external marker for plotting molecular weight size. Only complexes larger than 2,000 kDa were detected. (*B*) Experimental workflow used to purify FLAG-EVI1 protein complexes from SKOV3 cells. Proteomes of SKOV3 cells were metabolically labeled by incubation with light or heavy arginine and lysine isotopes. Nuclear lysates (5.6 mg) from light cells transfected with a FLAG plasmid and from heavy cells transfected with a FLAG-EVI1 plasmid were then separately subjected to immunoprecipitation with a FLAG antibody conjugated to agarose beads. The beads were combined in a 1:1 ratio during the washes. SDS eluates were subsequently separated by SDS/PAGE, digested with trypsin, and analyzed by using a nanoLC Orbitrap MS analyzer. After protein identification and quantitation, relative protein abundance in light and heavy was normalized. (*C*) Distribution of the ratio of heavy/light protein. Proteins associated with a heavy:light ratio of more than 3:1 were considered to be significantly enriched and potential EVI1 binding partners. The pie chart represents the proportion of previously known and newly identified EVI1 interacting proteins. (*D*) Protein domains significantly enriched within EVI1 binding partners obtained by using DAVID Bioinformatics.

with SILAC and other experimental results. Peptides from two previously known EVI1-associated proteins CTBP1 (11, 24) and CTBP2 (25), were consistently found bound to the EVI1 CTBP consensus binding motifs located between amino acids 553 to 557 and 584 to 588 (Fig. 3*A*). Remarkably, four other EVI1 interacting partners from our experiments (Dataset S1 and Fig. S2*C*) (18) were identified by yeast two-hybrid screening, including the JUN oncogene, two subunits of the PP1α protein phosphatase [protein phosphatase 1, regulatory subunit 9A (PPP1R9A) and protein phosphatase 1, regulatory subunit 9B (PPP1R9B)], and polymerase I and transcript release factor (PTRF), a protein known to terminate transcription by RNA polymerase I. Interestingly, 94.1% of the direct interactions between EVI1 baits and preys mapped outside of the two zinc finger domains and the C-terminal acidic region. Preys were mostly associated with the EVI1 repressor domain (27.4%) and the region located between the first zinc finger domain and the CTBP motifs (66.7%; Fig. 3*B*). Only one interaction, involving the coactivator CBP (26), has been previously linked to the EVI1 region located between amino acids 240 and 547. Our data suggest that many more interactions are likely to be associated with this region.

Classification of EVI1 Binding Partners Based on Known Protein Interactions. The organization and visualization of protein–protein interaction networks is critical for the biological interpretation of proteomics data. To identify the known protein interactions for our list of EVI1 binding partners, we used the Search Tool for the Retrieval of Interacting Genes/Proteins (STRING) database, which we restricted to protein–protein interactions that are based on experimental knowledge (Fig. S4). Subsequent functional clustering analyses by Database for Annotation, Visualization, and Integrated Discovery (DAVID) using all nuclear proteins as background identified several biological processes that were significantly enriched among the EVI1 binding partners. Not surprisingly, one of the major clusters contained proteins involved in the regulation of transcription (P = 0.0019; Fig. 4*A*). In these experiments, 13 TFs were identified that form complexes with EVI1 (Dataset S1 and Fig. 2*A*). Corepressors and coactivators of transcription were part of these interaction networks (Fig. 4*A*), consistent with the known dynamic action of EVI1 on transcriptional regulation (13, 15). We also found four proteins associated with EVI1 that regulate transcriptional initiation or termination. In addition, we identified enriched numbers of proteins involved in chromatin remodeling (P = 0.0003) and chromatin modification (P = 0.006; Fig. 4*B*), confirming that EVI1 regulates transcription in a more sustained manner by recruiting higher-order chromatin remodeling complexes. Indeed, EVI1 interacted with regulators of histone acetylation, deacetylation, and methylation, and members of the switch/sucrose nonfermentable (SWI/SNF) complex (Fig. 4*B*). More surprisingly, we found a highly significant enrichment (P = 0.002) for proteins involved in DNA damage repair (Fig. S5*A*). Other significant but smaller clusters included proteins involved in DNA recombination (P = 0.0003), regulation of cell cycle (P = 0.004), and meiosis (P = 0.004; Fig. S5 *B*–*D*). A few reports have also mentioned oncogenic signaling pathways such as TGF-β (19) and JNK signaling (30) as acting upstream of or merging toward EVI1, consistent with the enriched number of EVI1 binding partners we identified that are associated with signal transduction (P = 0.0101). Further classification showed that these proteins belonged not only to

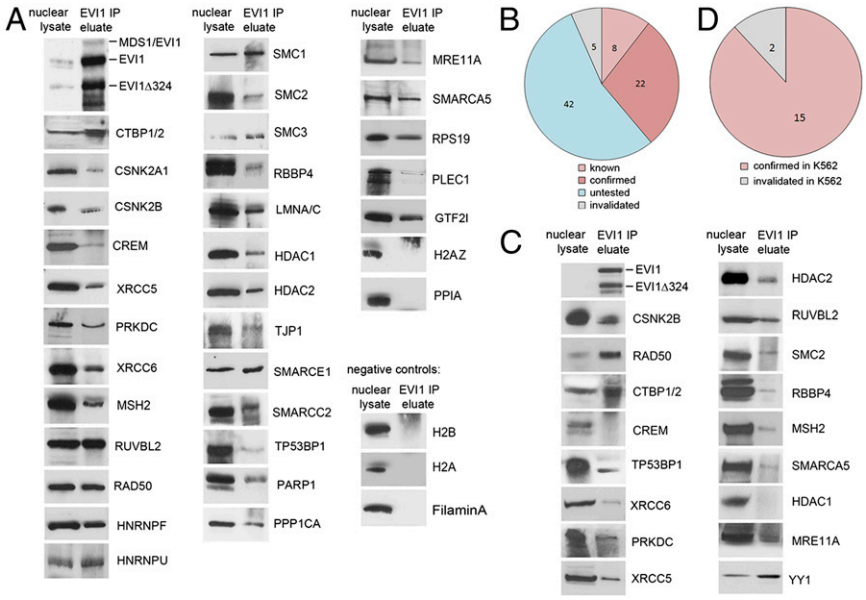

Fig. 2. Validation of proteomics data by coimmunoprecipitation of endogenous proteins. (*A*) Immunoprecipitation of EVI1 endogenous protein from SKOV3 nuclear extracts with EVI1 antibody. The EVI1 interaction partners identified by SILAC/MS-MS were subsequently detected in the immunoprecipitates by Western blotting by using the indicated antibodies. The left lane contains 5 μg of nuclear protein extract. The second lane was loaded with equal amounts of EVI1 immunoprecipitation eluates. (*B*) Proportion of EVI1 interacting proteins that were confirmed or invalidated by coimmunoprecipitation experiments with endogenous EVI1 in SKOV3 cells. A total of 81.5% of the previously unknown interactions assessed was validated. (*C*) The same experiment as in *A* was performed by using nuclear lysates from K562 leukemia cells. (*D*) Fraction of the 17 EVI1 interactions that were also confirmed in K562 protein extracts.

TGF-β and JNK signaling pathways, but also to WNT and RAS signaling pathways (Fig. S5*E*).

Identification of Functional Posttranslational EVI1 Modifications. Interestingly, our EVI1 interactome dataset contained a number of proteins that regulate posttranslational modifications, and suggested that EVI1 might be phosphorylated. For example, the protein Ser/Thr phosphatase-1α (i.e., PP1α) catalytic (PPP1CA) and regulatory (PPP1RGA, PPP1RGB) subunits were identified as EVI1 interacting proteins through SILAC MS and yeast two-hybrid experiments (Fig. 5*A*), suggesting that EVI1 is a direct substrate for this phosphatase. Moreover, EVI1 binding partners contained components of three different Ser/Thr kinases possibly directly promoting EVI1 phosphorylation. We identified all three subunits of CK2 [casein kinase 2, alpha 1 polypeptide (CSNK2A1); casein kinase 2, alpha 2 polypeptide (CSNK2A2); casein kinase 2, beta polypeptide (CSNK2B)], all three subunits of DNA-protein kinase [DNA-protein kinase (DNA-PK); protein kinase, DNA-activated, catalytic polypeptide (PRKDC); X-ray repair complementing defective repair in Chinese hamster cells (XRCC) 5, XRCC6], and CDC42 binding protein kinase-β (CDC42BPB) among the EVI1 interacting partners (Fig. 5*A*). To identify phosphorylation sites for these kinases on EVI1, we looked at the mass spectra and found three reliably phosphorylated EVI1 peptides: Ser436, Ser538 (Fig. 5*B*), and Ser858 or Ser860 (Fig. 5*C*). The spectrum of EVI1 peptide 849 to 862 did not make it possible to determine whether the phosphorylated serine was Ser858 or Ser860 (Fig. 5*B*). Other reports that used systematic MS approaches have also discovered EVI1 phosphorylation sites on Thr342, Ser860 (31), and Ser858 and Ser860 (32). We next determined whether any of these EVI1 phosphorylated sites belonged to CK2 or DNA-PK consensus motifs by using the Group-based Prediction System (version 2.1; Fig. 5*D*). The CDC42BPB consensus motif is unknown and could not be assessed. Ser538, Ser858, and Ser860 all contained a CK2 phosphorylation consensus motif, whereas Ser858 also contained a DNA-PK motif. The protein sequence at Ser538 carried a canonical CK2 recognition motif that is highly conserved in vertebrates. Orthologous sequences at Ser858/860 were less well conserved and carried a noncanonical CK2 recognition motif and a typical serine/threonine-glutamine DNA-PK motif (Fig. S6).

CK2 and PP1α Regulate EVI1 Phosphorylation on Ser538 and Ser858. The CSNK2A1 and CSNK2B components of CK2 ranked near the top of the SILAC MS list, at the fourth and sixth positions, respectively (heavy:light ratios of 16.84 and 10.53; Dataset S1). This provided evidence for a very specific interaction with EVI1 and suggested direct protein–protein interactions. The PPP1R9B PP1α regulatory subunit for which the yeast two-hybrid screens also confirmed a direct interaction, displayed a high heavy:light ratio of 7.86. To verify that CK2 could specifically phosphorylate endogenous EVI1 protein, we performed CK2 kinase assays on immunoprecipitated eluates from untransfected SKOV3 nuclear lysates (Fig. 5*E*). Specific incorporation of radiolabeled phosphates was identified for the two major EVI1 isoforms, EVI1 and EVIΔ324, attesting to their phosphorylation by recombinant CK2. A subsequent PP1α phosphatase assay dramatically reduced EVI1 phosphorylation, showing that PP1α could dephosphorylate the CK2-induced phosphorylation of EVI1. To confirm the possible CK2 phosphorylation site(s) (Fig. 5*D*), we mutated the FLAG-EVI1 plasmid to replace Ser538 with alanine (S538A), Ser858 with glycine (S858G), and/or Ser860 with alanine (S860A). These amino acid substitutions were meant to disrupt CK2-induced phosphorylation. We repeated the CK2 assay by using HeLa nuclear lysates that had been transfected with these different constructs (Fig. 5*F*). We used HeLa cells because they do not express endogenous EVI1 proteins that could interfere with the exogenously expressed FLAG-EVI1 proteins. The WT and S860A EVI1 proteins were strongly phosphorylated by CK2. However, the phosphorylation levels of the S538A and S858G mutants were impaired, demonstrating that Ser538 and Ser858 are the sites directly phosphorylated by CK2.

A

EVI1 implied minimal binding region	Prey	Number of occurances	Prey binding region
1-240	HCA127	1	1-141
180-380	LOC643491	1	114-253
241-495	AES(isoform a)	1	93-246
241-495	ARHGEF37	1	376-676
241-495	CHERP	1	469-885
241-495	HSF2(isoform b)	1	87-476
241-495	**JUN**	2	1-332
241-495	PKM2	1	393-532
241-495	PLXNB1(alt. transcript 2135)	1	1646-1738
241-495	RBM11	1	2-282
241-495	SH3PX1	1	548-596
241-495	SREBF1	1	251-422
241-495	SREBF2	1	1-362
241-495	TRIM11	2	1-469
241-495	TRIM26	1	59-303
241-495	TRIM58	1	1-238
241-495	TSNAX	1	1-207
241-495	VPS39	1	351-876
300-495	BAT3	5	174-300
300-495	FAM129B	2	420-555
300-495	GAS7	2	160-375
300-495	GTF3C2	10	70-225
300-495	PCBP2	15	147-262
300-495	**PPP1R9A**	2	693-788
300-495	UBAC1	2	23-166
300-495	**PPP1R9B**	3	664-812
300-500	BRD2	1	159-557
300-500	CAGE1	1	226-399
300-500	HSF2BP	2	26-335
300-500	PACSIN2	1	134-376
300-500	RB1CC1(isoform 2)	1	1355-1592
300-500	SF3B1	1	625-887
361-500	C14ORF145	6	403-617
361-560	**CTBP1**	1	3-353
496-716	AES(isoform c)	1	1-178
496-716	ANKRD11	1	2504-2665
496-716	**CTBP2**	1	20-446
496-716	LRC8	1	83-213
496-716	NMRAL1	1	1-237
496-716	OIP5	1	148-230
496-716	RNF31	1	554-1013
496-716	SOX13	1	1-234
496-716	TRAF4AF1	1	55-311
500-560	DZIP1(isoform 2)	7	86-232
540-740	EPB41L3	1	729-1042
540-740	GOLGA6L1	2	26-262
540-740	KIAA1529	1	438-719
645-716	**PTRF**	2	56-304
645-791	TPR	2	254-398
729-1051	MAGI3	2	411-664
896-1051	LNX2	2	224-691

B

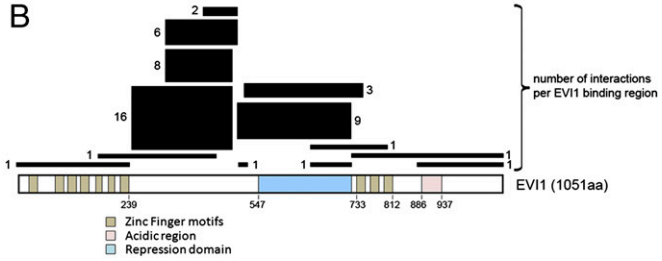

Fig. 3. Yeast two-hybrid screens identified 51 direct EVI1 binding proteins. (*A*) Results of the yeast two-hybrid screens performed with 18 EVI1 constructs and seven different libraries. The proteins labeled in bold are also found in the SILAC and immunoprecipitation experiments; they are direct EVI1 interacting proteins. (*B*) Mapping of all direct interactions identified on the EVI1 baits. Most of the direct binding occurred between the two zinc finger domains of EVI1.

Phosphorylation of EVI1 on Ser538 and Ser858 Modulates Its DNA Binding Activity and Oncogenic Potential. To better understand whether phosphorylation could affect EVI1 binding to other proteins, we performed coimmunoprecipitation experiments by using FLAG-EVI1 WT and mutant proteins. We could not detect any variation in the binding with 18 different interacting proteins between WT and mutant proteins. However, when we assessed the ability of EVI1 mutants S538A and S858G to bind to DNA probes containing the EVI1 N- or C-terminal GATA and E-twenty six (ETS)-like DNA-binding motifs, respectively, we noticed a reduction of binding for S538A and S858G to the C-terminal ETS-like probe (Fig. 6*A*). This provides evidence that disruption of these phosphorylation sites affects EVI1 binding to DNA. We next explored the effects of disruption of EVI1 phosphorylation at Ser538 and Ser858 on cellular functions regulated by EVI1. As expected (18), HeLa cells expressing FLAG-EVI1 displayed enhanced cell proliferation compared with the control cells. However, the activity of the S538A and S858G mutants on proliferation was reduced by 46.9% and 41.7%, respectively, compared with WT protein (Fig. 6*B*). Similar results were obtained in colony formation assays, in which the ability of the S538A and S858G mutant proteins to promote anchorage-independent cell growth was significantly impaired (Fig. 6*C*). Collectively, these results show that phosphorylation of EVI1 on Ser538 and Ser858 modulates its DNA-binding activity to the ETS-like DNA binding motif. Moreover, impairment of phosphorylation at these sites inhibits EVI1-induced cell proliferation and colony formation. These results are consistent with our previous findings showing that EVI1 target genes linked to the ETS-like motif are specifically enriched for genes that control cell proliferation (18).

We also explored the potential clinical relevance of these findings by looking at the correlation of gene expression between *EVI1* and the three CK2 subunits in tumors from ovarian carcinoma and patients with acute myeloid leukemia (AML) (33, 34). Our hypothesis was that tumors overexpressing *EVI1* might also favor the expression of the CK2 subunits, which could lead to an increase in EVI1 oncogenic activity. In support of this hypothesis, the heat maps representing the relative expression levels of *EVI1* (*MECOM* gene) and the three CK2 subunits in human patients tumors revealed a tendency for higher expression of CK2 subunits when *EVI1* was highly expressed (Fig. 6 *D* and *E*).

Discussion

Covalent posttranslational modifications modulate the activity of most eukaryote proteins (35). However, their presence on EVI1 and their functional consequences are still largely undefined. EVI1 acetylation has been previously described and could modulate EVI1 localization within nuclei (26) and improve its DNA-binding activity (36). We and others also identified several phosphorylation sites on EVI1 by MS, including phosphorylation of Ser338 (37), Thr342 (31), Ser436 (our data and refs. 37, 38), Ser538 (our data and refs. 37), and Ser858 or Ser860 (our data and refs. 27, 32). In this study, we also demonstrated that two serine residues on EVI1, Ser538 and Ser858, can be phosphorylated by CK2 and dephosphorylated by PP1α. Additional experiments with EVI1 mutants unable to be phosphorylated at these sites confirmed that EVI1 is regulated by multisite phosphorylation. EVI1 mutant proteins could not optimally bind DNA through their C-terminal zinc finger domain. As a consequence, the induction of cancer cell proliferation by EVI1 was impaired. This suggests that CK2 and PP1α signaling pathways could have opposing effects on EVI1 function whereby CK2-induced phosphorylation improves EVI1 oncogenic activity and PP1α-induced dephosphorylation reduces it. CK2 is a known oncogene whose activity is elevated in a large number of human tumors as a result of increased expression of its component proteins (39). CK2 therefore represents a potential new drug target for the treatment of EVI1-associated disease (40). Interestingly, other reports have identified a similar balance between the CK2 and PP1 pathways in the regulation of the IKAROS zinc finger TF (41, 42). However, unlike EVI1, IKAROS function was lost after CK2 phosphorylation and restored by PP1. This is consistent with the role of IKAROS as a tumor suppressor rather than an oncogene in hematological malignancies (43).

Interestingly, we also found that EVI1 can complex with RuvB-like 1 (RUVBL1) and RuvB-like 2 (RUVBL2) (also called Pontin and Reptin, respectively), which can associate with chromatin-remodeling complexes to regulate transcription, DNA damage

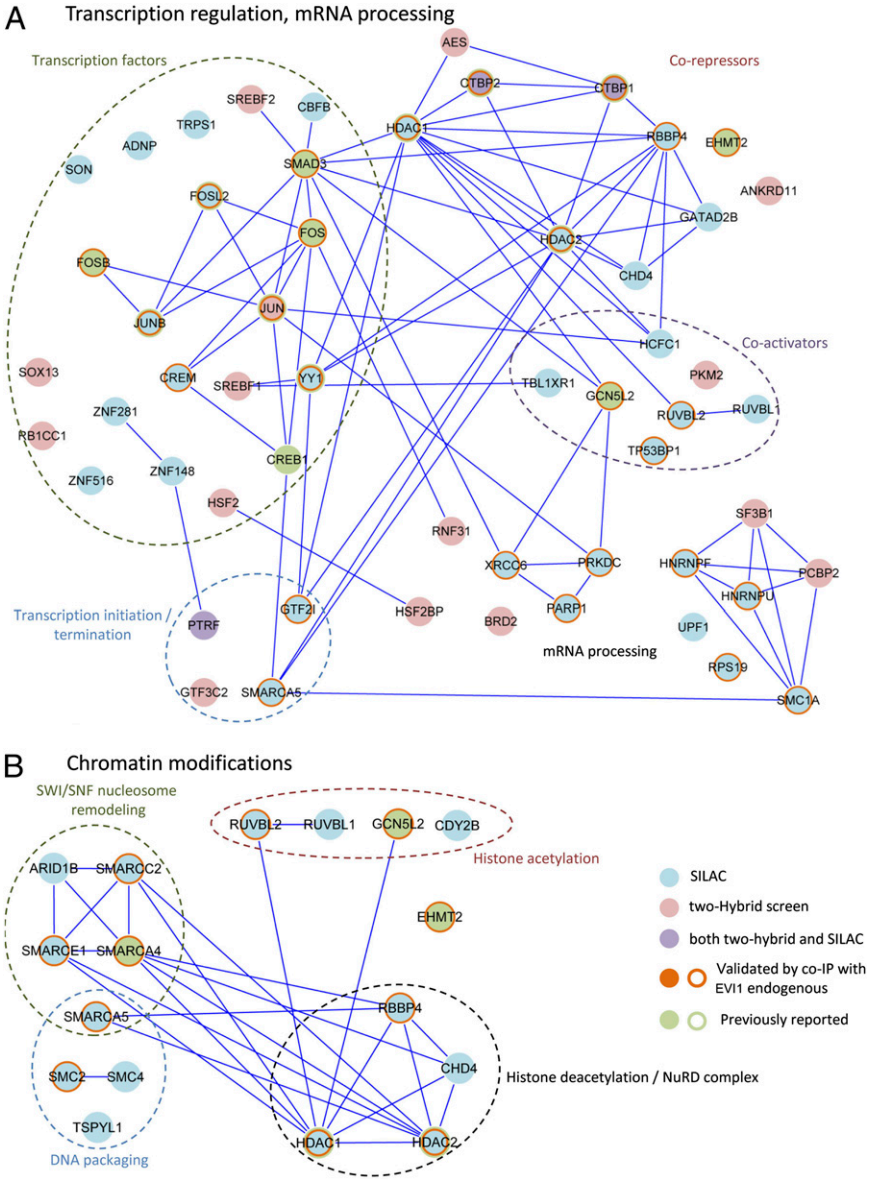

Fig. 4. EVI1-related protein interaction networks involved in transcriptional regulation and chromatin modification. The networks represent protein–protein interactions identified exclusively from STRING database (experimental knowledge-based). The proteins examined were the ones identified in the SILAC MS-based experiments (Dataset S1 and Fig. 3*A*) or those described in the literature as EVI1 binding partners. EVI1-associated protein networks correlated with (*A*) transcriptional regulation and (*B*) chromatin modification are represented.

repair, and telomerase activity (44). Pontin and Reptin are known to enhance the oncogenic functions of several TFs, including β-catenin and myelocytose gene (45, 46). We expect that similar mechanistic regulations could apply to EVI1. Additionally, a significantly enriched subset of EVI1 binding partners was identified that consisted of proteins involved in DNA damage repair and DNA recombination. These findings suggest a direct involvement of EVI1 in regulating genomic instability, which might help to explain the recently described role of EVI1 in the production of genetic alterations that drive malignant growth (47, 48).

Protein–protein interaction maps have proven to be very useful for understanding the biology and function of the molecules within them. Our characterization and classification of the EVI1 interactome have similarly provided important clues to better understand the molecular functions of EVI1. For example, our studies have shown that EVI1 is contained within very large protein complexes, which likely serve to integrate various different signals through the interaction of EVI1 with its many partner proteins. A few reports have mentioned oncogenic signaling pathways such as TGF-β (19) and JNK (30) as acting upstream of or merging toward EVI1. Consistent with this, our studies identified many TFs that associate with EVI1, including TFs involved in TGF-β and JNK signaling as well as WNT and RAS signaling. EVI1 thus appears to integrate signals from many different signal networks to regulate downstream transcriptional control and/or epigenetic modifications.

EVI1 oncogenic TF remained poorly characterized, despite its identification by retroviral mutagenesis screens in mice in 1988 (16, 17) and its proven clinical implication in various cancer types (1–10). To better understand its molecular functions in cancer progression, we have performed two studies based on genomics (ChIP-sequencing/microarray analyses) (18) and proteomics experiments in cancer cells. These two reports brought complementary information whereby the genomics

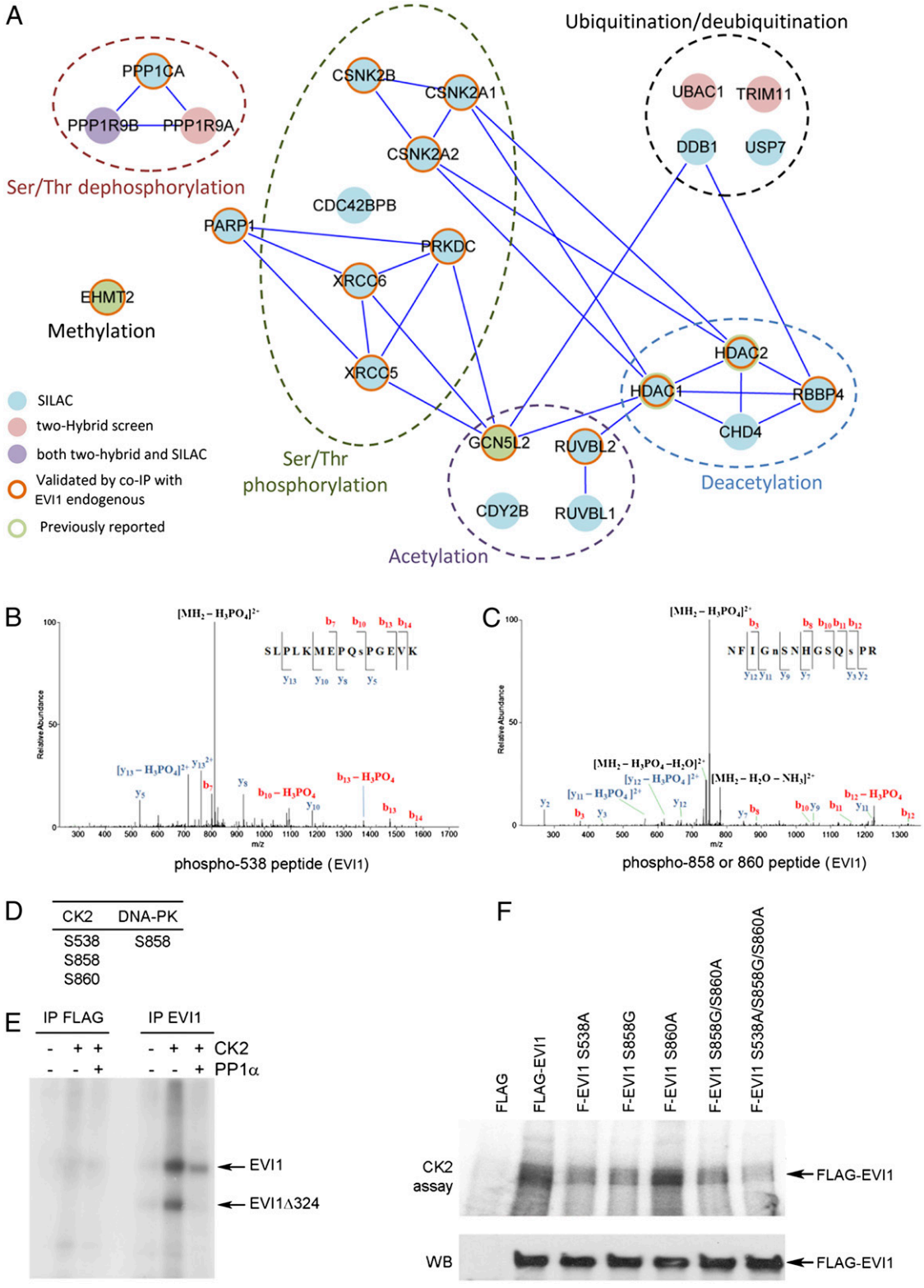

Fig. 5. EVI1 is phosphorylated by CK2 and dephosphorylated by PP1α. (*A*) Protein interaction networks for the EVI1-associated proteins directly involved in posttranslational protein modifications. All three subunits of the CK2, DNA-PK, and PP1α enzymes were identified by SILAC MS. (*B* and *C*) Mass spectra showing phosphorylation of EVI1 on Ser538 (*B*) and Ser858 or Ser860 (*C*). (*D*) EVI1 phosphorylation sites contain motifs for kinases found in complexes with EVI1 (by Group-based Prediction System). (*E*) CK2 kinase and PP1α phosphatase assays after immunoprecipitation of the EVI1 endogenous protein from SKOV3 nuclear lysates. (*F*) CK2 kinase assay after immunoprecipitation of the FLAG tag only, FLAG-EVI1 WT or FLAG-EVI1 mutant proteins from transfected HeLa nuclear lysates (*Upper*). A control Western blot (*Lower*) confirmed that equal amounts of FLAG-EVI1 protein were expressed in HeLa nuclear lysates.

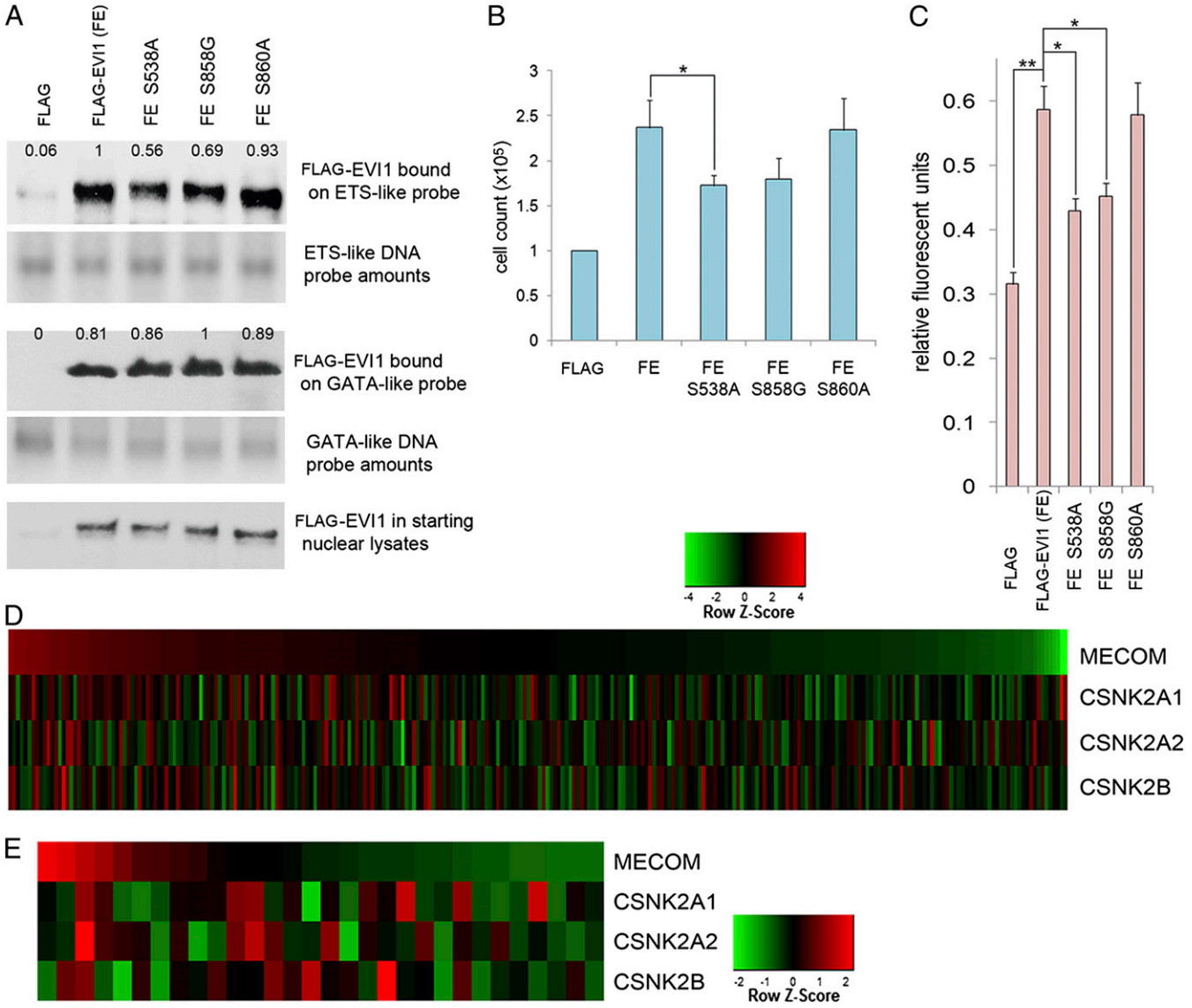

Fig. 6. Phosphorylation of Ser538 and Ser858 modulates EVI1 DNA-binding and oncogenic activity. HeLa cells were transfected with the indicated plasmids. (*A*) In vitro DNA binding assay of EVI1 WT and mutant proteins. Biotin-labeled DNA probes carrying the EVI1 N- or C-terminal zinc finger domains were incubated with nuclear lysates. Western blot analysis with EVI1 antibody after streptavidin pull-down revealed the amount of FLAG-EVI1 (FE) proteins associated with the DNA probes. The amount of DNA probes and FLAG-EVI1 proteins in starting materials are shown as loading controls. Quantification of the FLAG-EVI1 bound to the probes was obtained by ImageJ and normalized to the DNA probe amounts. (*B*) Reduced ability of EVI1 S538A and S858G mutants to induce HeLa cell growth. The total cell number was counted 3 d after transfection. (*C*) Colony formation by EVI1 is impaired for the two mutant forms. Transfected HeLa cells were grown in soft agar for 7 d. The final amount of cells was detected by using a fluorimetric assay. (*B* and *C*) Data are the average of three independent experiments. Values are presented as mean ± SEM (*$P < 0.05$ and **$P < 0.01$, Student *t* test). (*D* and *E*) Heat maps showing the expression of *MECOM* (*EVI1*) and three CK2 subunits from selected patient tumors. Higher expression of MECOM associates with stronger expression of CK2 subunits. (*D*) Expression data from 285 ovarian carcinoma samples (33). (*E*) Expression data from 30 AML tumors expressing *EVI1* (34).

experiments rather identified EVI1 genome-wide occupancy, domain-specific DNA binding features, and target genes, and unraveled functional cooperative interaction with activator protein 1 TF (18). The present proteomics analyses confirm the direct interaction between EVI1 and AP1, and also characterize EVI1 regulatory protein networks and fine transcriptional regulations through functional posttranslational modifications. Altogether, these results from proteomics and genomics experiments provide a deep understanding of EVI1 role in cancer and of its interaction with other oncogenes and pathways.

Materials and Methods

More details of study methods are provided in *SI Materials and Methods*.

Cell Culture, Transfections, and SILAC. SKOV3 (HTB-77; American Type Culture Collection) and HeLa (CCL-2; American Type Culture Collection) cells were maintained in DMEM and 10% FBS. K562 (CCL-243; American Type Culture Collection) cells were cultured in RPMI and 10% (vol/vol) FBS. HeLa and SKOV3 cells were transfected with Lipofectamine (Invitrogen) or Fugene6 (Roche), respectively. For SILAC, SKOV3 cells were grown in SILAC DMEM and 10% dialyzed FBS supplemented with L-arginine and L-lysine for the light culture or with L-arginine (U-13C6) and L-lysine (U-13C6) for the heavy culture (Thermo Scientific). The cells were used after six doublings in SILAC media to allow for full metabolic incorporation.

Cloning and EVI1 Mutagenesis. EVI1 cDNA was subcloned into the pENTR/D-TOPO vector (Invitrogen) from a human erythroleukemia cell line leukemia cell cDNA library. The entire EVI1 sequence (3,153bp) was similar to National Center for Biotechnology Information Reference Sequence NM_005241.

EVI1 cDNA was transferred into a Gateway pcDNA-DEST53 vector (Invitrogen) for which the GFP tag had been replaced with a FLAG tag (N terminus). Mutations in the FLAG-EVI1 plasmid were generated by site-directed mutagenesis. The pcDNA3 plasmid in which one FLAG tag was inserted was used as a control plasmid expressing the FLAG tag only.

Extraction of Nuclear Proteins, Immunoprecipitations, and Western Blotting. Extraction of nuclear proteins is described in *SI Materials and Methods*. For the detection of EVI1 interacting proteins by MS, 5 mg of nuclear proteins from SKOV3 heavy or light cells were used. The lysates were precleared with A/G beads (Santa Cruz). Thirty microliters of EZview Red Anti-FLAG M2 Affinity Gel (Sigma) were added to each lysate for immunoprecipitation. The beads were washed, combined, and washed three more times before elution. The eluate was separated on SDS/PAGE gels. A similar procedure was used on 11.8 mg SKOV3 nuclear extract for the identification of phosphorylated EVI1 peptides. For the coimmunoprecipitations with endogenous proteins, 28 μg of nuclear proteins from SKOV3 or K562 cells were used per immunoprecipitation with Dynabeads protein G (Invitrogen) coupled with EVI1 antibody (no. 2593; Cell Signaling). After washes and SDS elution, immunoblotting analyses revealed the presence EVI1 interacting proteins.

MS of Proteins. Eluted EVI1 protein complexes were separated by SDS/PAGE and digested with trypsin (49). Peptide identification was performed by using an LTQ-Orbitrap mass spectrometer (Thermo Fisher Scientific). Full-scan MS spectra were acquired with a resolution of 60,000 in the Orbitrap analyzer. For every full scan, the 10 most intense ions were fragmented in the linear ion trap. Raw data were processed and analyzed by using the MaxQuant software using default settings and searched with the Mascot search engine against the human International Protein Index database 3.52. For identifying sites of phosphorylation eluted EVI1 immunoprecipitate (non-SILAC) was separated by 1D gel and the band corresponding to EVI1 was subjected to MS analysis as described earlier. Scaffold software was used to validate MS/MS-based peptide and protein identifications. Protein identifications were accepted at probability greater than 95% as assigned by Protein Prophet algorithm (50). All phosphorylation peptides of EVI1 were manually validated.

Gel Filtration Chromatography. Nuclear extracts from untransfected SKOV3 cells were resuspended in 150 mM NaCl, 0.13 mM $CaCl_2$, 10 mM Tris/CL, pH 7.5, 5 mM $MgCl_2$, homogenized, and incubated with DNaseI for 2 h at 4 °C (Roche). The lysate was cleared through a 22-μm filter to remove particulate matter. Fifty micrograms of cleared lysate was applied to a Precision Column 3.2/30 Superdex 200 column (Amersham Biosciences) equilibrated with the same buffer in a SMART system (Amersham Biosciences) at a flow rate of 25 μL/min. Fractions of 15 μL were collected and resolved on SDS/PAGE, and the presence of EVI1 was identified by Western blot.

Yeast Two-Hybrid Screens. ProNet from Myrexis, an automated high-throughput yeast two-hybrid research system (29), was used for the identification and characterization of direct EVI1–protein interactions with a lower rate of false-positive findings. A total of 18 baits for EVI1 were screened, and 11 of them (Fig. S3) gave rise to specific interactions after searching seven different libraries (breast cancer/prostate cancer, prostate cancer, brain, stem cell, testis, lung, and spleen libraries).

Protein Kinase and Phosphatase Assays. EVI1 or the FLAG M2 (Sigma) antibodies were captured on Dynabeads protein G before incubation with 200 μg SKOV3 or transfected HeLa nuclear lysates. The beads were washed two times with CK2 buffer (20 mM Tris·HCl, pH 7.5, 50 mM KCl, 10 mM $MgCl_2$, 25 mM β-glycerol phosphate, 1 mM DTT). Recombinant CK2 20 U (Calbiochem) supplemented with 5 μM cold ATP and 20 μCi γATP were added to the beads for 15 min. The eluates were separated by SDS/PAGE before revelation. The PP1 phosphatase assay was performed on beads following the 15-min incubation with CK2. The beads were washed three times with Buffer J (150 mM NaCl, 0.1% Tween-20, 50 mM Hepes, pH 7.3) and twice with NEBuffer for Protein MetalloPhosphatases (NEB). The beads were incubated with $MnCl_2$ and 15 U of PP1α phosphatase (P0754; NEB), after which two washes with NEBuffer for Protein MetalloPhosphatases and three washes with Buffer J were performed before elution.

Proliferation and Colony Formation Assays. The proliferation assay was carried out by using HeLa cells transfected with the indicated plasmids in 24-well plates. The cells were counted 3 d after transfection. Colony formation assays (Cell Biolabs) were carried out as indicated by the manufacturer. One day after transfection, 5,000 HeLa cells suspended in agar were added in each well. The quantification of anchorage-independent growth was measured 7 d later.

Biotin-Labeled DNA Probe Binding Assays. A previously published protocol (51) was adapted to a small-scale analysis. Biotin-labeled DNA probes were captured on MyOne Dynabeads T1, blocked, and washed. Fifteen microliters of 8 mg/mL nuclear lysate was added to the beads, and incubation was performed overnight at 4 °C. Two washes were performed before the beads were eluted. The eluate was used for immunoblotting analysis.

Computational Analyses. To perform the gene-annotation enrichment analyses, the EVI1-associated protein IDs were uploaded to DAVID Bioinformatics version 6.7 (52, 53). The list of all human genes was used as default background in Fig. 1*D*. In other enrichment analyses, the list of all proteins with nuclear localization was used as background. The analyses were performed by using protein domains, Gene Ontology Term (GOTERM), Protein Analysis Through Evolutionary Relationships (PANTHER), and Kyoto Encyclopedia of Genes and Genomes (KEGG) pathway. To design the protein networks of EVI1 binding partners, we obtained all interactions from the STRING database. Cytoscape was used to filter these interactions, and we kept only the protein–protein interactions based on experimental knowledge (Cytoscape code MI:0046). Microarray data were ordered by mean of MECOM expression by using 277 patients with ovarian cancer (33) and 30 patients with AML (34), respectively. The 30 patients with AML were selected based on greater than quartile global expression levels of MECOM.

ACKNOWLEDGMENTS. We thank Yong Jeffrey for sharing his expertise for the size exclusion chromatography experiments, Sheena Wee and Kelly Hogue for their input in MS data analyses, and Ahmed Sayadi for drawing the networks. This study was supported by the Agency for Science, Technology and Research (Singapore) and Cancer Prevention and Research Institute of Texas (CPRIT; N.G.C. and N.A.J.). N.G.C. and N.A.J. are CPRIT Scholars in Cancer Research.

1. Goyama S, Kurokawa M (2009) Pathogenetic significance of ecotropic viral integration site-1 in hematological malignancies. *Cancer Sci* 100(6):990–995.
2. Lugthart S, et al. (2008) High EVI1 levels predict adverse outcome in acute myeloid leukemia: Prevalence of EVI1 overexpression and chromosome 3q26 abnormalities underestimated. *Blood* 111(8):4329–4337.
3. Ogawa S, et al. (1996) Increased Evi-1 expression is frequently observed in blastic crisis of chronic myelocytic leukemia. *Leukemia* 10(5):788–794.
4. Bei JX, et al. (2010) A genome-wide association study of nasopharyngeal carcinoma identifies three new susceptibility loci. *Nat Genet* 42(7):599–603.
5. Brooks DJ, et al. (1996) Expression of the zinc finger gene EVI-1 in ovarian and other cancers. *Br J Cancer* 74(10):1518–1525.
6. Choi YW, et al. (2007) Comparative genomic hybridization array analysis and real time PCR reveals genomic alterations in squamous cell carcinomas of the lung. *Lung Cancer* 55(1):43–51.
7. Starr TK, et al. (2009) A transposon-based genetic screen in mice identifies genes altered in colorectal cancer. *Science* 323(5922):1747–1750.
8. Yokoi S, et al. (2003) TERC identified as a probable target within the 3q26 amplicon that is detected frequently in non-small cell lung cancers. *Clin Cancer Res* 9(13):4705–4713.
9. Nanjundan M, et al. (2007) Amplification of MDS1/EVI1 and EVI1, located in the 3q26.2 amplicon, is associated with favorable patient prognosis in ovarian cancer. *Cancer Res* 67(7):3074–3084.
10. Osterberg L, et al. (2009) Potential predictive markers of chemotherapy resistance in stage III ovarian serous carcinomas. *BMC Cancer* 9:368.
11. Hirai H, Izutsu K, Kurokawa M, Mitani K (2001) Oncogenic mechanisms of Evi-1 protein. *Cancer Chemother Pharmacol* 48(suppl 1):S35–S40.
12. Nucifora G, Laricchia-Robbio L, Senyuk V (2006) EVI1 and hematopoietic disorders: History and perspectives. *Gene* 368:1–11.
13. Wieser R (2007) The oncogene and developmental regulator EVI1: Expression, biochemical properties, and biological functions. *Gene* 396(2):346–357.
14. Kilbey A, Bartholomew C (1998) Evi-1 ZF1 DNA binding activity and a second distinct transcriptional repressor region are both required for optimal transformation of Rat1 fibroblasts. *Oncogene* 16(17):2287–2291.
15. Métais JY, Dunbar CE (2008) The MDS1-EVI1 gene complex as a retrovirus integration site: Impact on behavior of hematopoietic cells and implications for gene therapy. *Mol Ther* 16(3):439–449.
16. Morishita K, et al. (1988) Retroviral activation of a novel gene encoding a zinc finger protein in IL-3-dependent myeloid leukemia cell lines. *Cell* 54(6):831–840.
17. Mucenski ML, et al. (1988) Identification of a common ecotropic viral integration site, Evi-1, in the DNA of AKXD murine myeloid tumors. *Mol Cell Biol* 8(1):301–308.
18. Bard-Chapeau EA, et al. (2012) Ecotopic viral integration site 1 (EVI1) regulates multiple cellular processes important for cancer and is a synergistic partner for FOS protein in invasive tumors. *Proc Natl Acad Sci USA* 109(6):2168–2173.

19. Kurokawa M, et al. (1998) The oncoprotein Evi-1 represses TGF-beta signalling by inhibiting Smad3. *Nature* 394(6688):92–96.
20. Laricchia-Robbio L, et al. (2006) Point mutations in two EVI1 Zn fingers abolish EVI1-GATA1 interaction and allow erythroid differentiation of murine bone marrow cells. *Mol Cell Biol* 26(20):7658–7666.
21. Laricchia-Robbio L, Premanand K, Rinaldi CR, Nucifora G (2009) EVI1 Impairs myelopoiesis by deregulation of PU.1 function. *Cancer Res* 69(4):1633–1642.
22. Senyuk V, et al. (2007) Repression of RUNX1 activity by EVI1: A new role of EVI1 in leukemogenesis. *Cancer Res* 67(12):5658–5666.
23. Ong SE, et al. (2002) Stable isotope labeling by amino acids in cell culture, SILAC, as a simple and accurate approach to expression proteomics. *Mol Cell Proteomics* 1(5): 376–386.
24. Izutsu K, et al. (2001) The corepressor CtBP interacts with Evi-1 to repress transforming growth factor beta signaling. *Blood* 97(9):2815–2822.
25. Turner J, Crossley M (1998) Cloning and characterization of mCtBP2, a co-repressor that associates with basic Krüppel-like factor and other mammalian transcriptional regulators. *EMBO J* 17(17):5129–5140.
26. Chakraborty S, Senyuk V, Sitailo S, Chi Y, Nucifora G (2001) Interaction of EVI1 with cAMP-responsive element-binding protein-binding protein (CBP) and p300/CBP-associated factor (P/CAF) results in reversible acetylation of EVI1 and in co-localization in nuclear speckles. *J Biol Chem* 276(48):44936–44943.
27. Chen GI, Gingras AC (2007) Affinity-purification mass spectrometry (AP-MS) of serine/threonine phosphatases. *Methods* 42(3):298–305.
28. Harfe BD, Jinks-Robertson S (2000) DNA mismatch repair and genetic instability. *Annu Rev Genet* 34:359–399.
29. Garrus JE, et al. (2001) Tsg101 and the vacuolar protein sorting pathway are essential for HIV-1 budding. *Cell* 107(1):55–65.
30. Kurokawa M, et al. (2000) The evi-1 oncoprotein inhibits c-Jun N-terminal kinase and prevents stress-induced cell death. *EMBO J* 19(12):2958–2968.
31. Chen RQ, et al. (2009) CDC25B mediates rapamycin-induced oncogenic responses in cancer cells. *Cancer Res* 69(6):2663–2668.
32. Matsuoka S, et al. (2007) ATM and ATR substrate analysis reveals extensive protein networks responsive to DNA damage. *Science* 316(5828):1160–1166.
33. Tothill RW, et al.; Australian Ovarian Cancer Study Group (2008) Novel molecular subtypes of serous and endometrioid ovarian cancer linked to clinical outcome. *Clin Cancer Res* 14(16):5198–5208.
34. Valk PJ, et al. (2004) Prognostically useful gene-expression profiles in acute myeloid leukemia. *N Engl J Med* 350(16):1617–1628.
35. Mann M, Jensen ON (2003) Proteomic analysis of post-translational modifications. *Nat Biotechnol* 21(3):255–261.
36. Shimahara A, Yamakawa N, Nishikata I, Morishita K (2010) Acetylation of lysine 564 adjacent to the C-terminal binding protein-binding motif in EVI1 is crucial for transcriptional activation of GATA2. *J Biol Chem* 285(22):16967–16977.
37. Choudhary C, et al. (2009) Mislocalized activation of oncogenic RTKs switches downstream signaling outcomes. *Mol Cell* 36(2):326–339.
38. Huttlin EL, et al. (2010) A tissue-specific atlas of mouse protein phosphorylation and expression. *Cell* 143(7):1174–1189.
39. Ruzzene M, Pinna LA (2010) Addiction to protein kinase CK2: A common denominator of diverse cancer cells? *Biochim Biophys Acta* 1804(3):499–504.
40. Sarno S, Pinna LA (2008) Protein kinase CK2 as a druggable target. *Mol Biosyst* 4(9): 889–894.
41. Gurel Z, et al. (2008) Recruitment of ikaros to pericentromeric heterochromatin is regulated by phosphorylation. *J Biol Chem* 283(13):8291–8300.
42. Popescu M, et al. (2009) Ikaros stability and pericentromeric localization are regulated by protein phosphatase 1. *J Biol Chem* 284(20):13869–13880.
43. Dovat S, Song C, Payne KJ, Li Z (2011) Ikaros, CK2 kinase, and the road to leukemia. *Mol Cell Biochem* 356(1-2):201–207.
44. Grigoletto A, Lestienne P, Rosenbaum J (2011) The multifaceted proteins Reptin and Pontin as major players in cancer. *Biochim Biophys Acta* 1815(2):147–157.
45. Huber O, et al. (2008) Pontin and reptin, two related ATPases with multiple roles in cancer. *Cancer Res* 68(17):6873–6876.
46. Jha S, Dutta A (2009) RVB1/RVB2: Running rings around molecular biology. *Mol Cell* 34(5):521–533.
47. Dunbar CE, Larochelle A (2010) Gene therapy activates EVI1, destabilizes chromosomes. *Nat Med* 16(2):163–165.
48. Stein S, et al. (2010) Genomic instability and myelodysplasia with monosomy 7 consequent to EVI1 activation after gene therapy for chronic granulomatous disease. *Nat Med* 16(2):198–204.
49. Shevchenko A, Tomas H, Havlis J, Olsen JV, Mann M (2006) In-gel digestion for mass spectrometric characterization of proteins and proteomes. *Nat Protoc* 1(6): 2856–2860.
50. Nesvizhskii AI, Keller A, Kolker E, Aebersold R (2003) A statistical model for identifying proteins by tandem mass spectrometry. *Anal Chem* 75(17):4646–4658.
51. Mittler G, Butter F, Mann M (2009) A SILAC-based DNA protein interaction screen that identifies candidate binding proteins to functional DNA elements. *Genome Res* 19(2): 284–293.
52. Dennis G, Jr., et al. (2003) DAVID: Database for Annotation, Visualization, and Integrated Discovery. *Genome Biol* 4(5):3.
53. Huang W, Sherman BT, Lempicki RA (2009) Systematic and integrative analysis of large gene lists using DAVID bioinformatics resources. *Nat Protoc* 4(1):44–57.